www.lajss.org
Latin American Journal of Solids and Structures 3 (2006) 3–20

The nanoclay influence on impact response of laminated plates

Antonio Avila[a,*], Horácio V. Duarte[b] and Marcelo I. Soares[a]

[a]Universidade Federal de Minas Gerais, Department of Mechanical Engineering, NanoComposites Laboratory, 6627 Antonio Carlos Avenue, Belo Horizonte, Minas Gerais 31270-901, Brazil – Phone: +55 31 3499-5238, FAX: + 55 31 3443-3783
[b]Universidade Federal de Minas Gerais, Department of Mechanical Engineering, Vibration and Acoustics Laboratory, 6627 Antonio Carlos Avenue, Belo Horizonte, Minas Gerais 31270-901, Brazil – E-mail: horacio@demec.ufmg.br

Abstract

Protection of industrial, military and civil engineering structures against impact loadings have gained a lot of attention, specially after the 9/11 terrorist attacks. An economical and viable option to conventional and high cost ballistic materials is the use of fiber glass/epoxy composites, but for impact applications their toughness still has to be enhanced. Studies developed by Yasmin et al. and Isik et al. demonstrated that by adding a small amount of nanoclays into epoxy systems, a sensible increase on mechanical properties can be obtained. To investigate how the plate impact strength is affected by the presence of nanoclays, a set of fiber glass-epoxy-nanoclay laminate composites with 16 layers and 65% fiber volume fraction is manufactured by vacuum assisted wet lay-up. Fibers have a plain-weave configuration with density of 180 g/m^2, while the epoxy resin system is made of diglycidyl ether of bisphenol *A* resin with aliphatic amine as the curing agent. The nanoclay (Nanomer I30E) is an organically modified montmorillonite ceramic and it is exfoliated into the epoxy system in a 1%, 2%, 5% and 10% ratio in weight with respect to the matrix. The square plates have a 150 mm edge and thickness of 2.4 mm. The methodology used for the impact test is based on the ASTM D5628-01 standard. The results have shown that for the four edges clamped condition not only the delamination phenomenon is reduced but also the damping is increased during the rebounds. However, the most favorable nanoclay concentration seems to be close to 5%. This can be due to the vibration mode superposition associated to a stiffness enhancement.

Keywords: Low velocity impact, natural frequency, damping coefficient, nanoComposites, nanoclay exfoliation.

1 Introduction

The usage of high performance polymeric composites is a valuable alternative to conventional materials due to their high specific mechanical properties, i.e. stiffness-to-weight and strength-to-weight, tailor-ability and damage tolerance. These composite materials and/or structures

*Corresp. author Email: aavila@netuno.lcc.ufmg.br Received 29 Sep. 2005; In revised form 6 Feb. 2006

during their service life undergo various loading conditions. Among them, the most critical condition is the impact loadings due to the laminated nature of these structures. According to Luo et al. [25], the damage in composite structures resulting from impact events is one of the most important aspects to be considered in the design and applications of composite materials. Impact events, however, can be classified according to the impact velocity, i.e. low and high velocities. As mentioned by Naik and Shrirao [28], low velocity impact events occur when the contact period of the impactor is longer than the time period of the lowest vibration mode. In this case, the support conditions are critical as the stress waves generated outward from the impact point have time to reach the edges of the structural element, causing its full-vibration response. Still, in high velocity impact, the contact period of the impactor is much smaller than the time period of the lowest vibration mode of the structure. As a consequence, the response of the structural element is governed by the local behavior of the material in the neighborhood of the impacted zone, the impact response of the element being generally independent of its support conditions.

As stated by Hu et al. [16], low velocity impacts on laminates produce multiple stacked delaminations at a number of interfaces through the thickness of the composite laminates. These inter-ply failures bring a significant reduction in strength and stiffness of the laminates. Hence, understanding the impact damage mechanism is essential to improve the composite materials performance. Experimental studies on low velocity impact developed by Liu et al. [23] showed that the thickness has a greater influence on impact perforation resistance than on the in-plane dimensions. While in Belingardi and Vadori [5], the energy absorption was evaluated considering the damage degree and the saturation impact energy which allowed corroborating the relationships between thickness and impact perforation resistance. By performing a finite element analysis associated to experimental data, Moura and Gonçalves [27] were able to create an accurate progressive damage model and successfully simulate the interaction between crack and delamination into low velocity impact problems. Meanwhile, according to Mines et al. [26], for high velocity impact, the perforation mechanics depend on the fiber type and volume fraction, the matrix, the stacking sequence, the size and initial kinetic energy of the impactor. Moreover, Cheng et al. [7] had demonstrated that penetration process can be broken down into three sequential stages: (i) punching; (ii) fiber breaking; and (iii) delamination. They even tried to model the perforation phenomenon by considering a failure criteria based on these three stages. Although their model presented good correlations against experimental results they were limited to a 2-D axi-symmetric geometry and it was based on a continuum approach.

Gu [12], Potti and Sun [30], and Abrate [2] are among those researchers that have elaborated more refined perforation models to evaluate the perforation performance. The model created by Gu [7] took into consideration not only the energy conservation laws but also the absorbed kinetic energy of the projectile. By adding the composite strain energy to his model, Gu [12] was able to estimate the progressive damage and delaminations caused by the high velocity impact. Potti and Sun [30], however, considered the use of the dynamic response model along with the critical deflection criterion to analyze the high velocity impact and perforation. They

concluded that the delaminated area increases with the velocity up to the penetration ballistic limit, as expected. However, beyond this limit, the delamination area decreases with the increase of velocity. Their model was able to capture this phenomenon with accuracy. Furthermore, Abrate [2] mentioned that compressive strains in high velocity impact situations are inversely proportional to the stress wave propagation through the composite thickness. Still, in a small area near the impactor, this stress wave reaches the speed of sound, which supports the results presented by Potti and Sun [30].

In all cases, low or high impact velocities, the key issue in the design of composite structures is the damage tolerance of each component, i.e. fibers and matrix. According to da Silva Junior et al. [18], the use of aramid reinforced composites presents one of the best protections to weight ratio for impact applications. However, the high cost of these fibers is a disadvantage. One viable substitute to aramid fibers is the use of carbon fibers. Nevertheless, as mentioned by Davies and Zhang [9], carbon fibers epoxy composites have an elastic behavior, but they are also brittle. Therefore, they suggested the use of fiber glass reinforced as carbon fiber replacement. Yet, fiber glass composite toughness is highly dependent on strain rate damage and the matrix behavior itself. A possible solution for this problem is to enhance the matrix toughness. This goal can be obtained by substituting the net epoxy system by a epoxy-nanoclay system.

As stated by Liu et al. [24], the use of nanoclays as reinforcement of polymer systems was introduced by the Toyota Research group in the early 90's. By that time, nylon-6 based clay nanocomposites were synthesized. They concluded that nanoclays not only influenced the crystallization process but they were also responsible for morphological changes. Liu et al. [24] reported that there was an increase in storage elastic modulus of 100% when clay content was up to 8 wt% in comparison with net nylon 11. Yie et al. [37] demonstrated that for polystyrene-montmorillonite nanocomposites, the glass transition temperature was higher than the virgin polystyrene. In both cases, thermoplastics were used as matrices. Different researchers, however, decided to study the influence of nanoparticles in epoxy systems due to their large use by the composite structures industry.

Yasmin et al. [35] were among those researchers who studied the effect of nanoparticles (organically modified montmorillonite - Cloisite 30B) into epoxy systems. By varying the amount of Cloisite 30B, in weight from 1% up to 10%, they found an increase in the elastic moduli to a maximum of 80%. A more interesting result using nanoparticles into epoxy system was reported by Isik et al. [17]. They concluded both stiffness and toughness were enhanced by nanoparticles. However, for their binary system, resin - diglycidyl ether of bisphenol A and cure agent - triethylenetetramine, the maximum impact strength was obtained at 1% in weight of montmorillonite content. The difference between Yasmin et al. [35] and Isik et al. [17] results can be attributed to the mixing process, shear mixing in Yasmin's case and direct mixing for Isik's conditions.

A more comprehensive study on clay-epoxy nanocomposites was performed by Haque and Shamsuzzoha [14], since not only mechanical properties but also thermal properties were evaluated. Their main conclusions were that thermo-mechanical properties mostly increase at low

clay loadings ($\sim$ 1-2% in weight) but decrease at higher clay loadings ($\geq$ 5% in weight). In addition, the uses of nanoclays also decrease the coefficient of thermal expansion (CTE). They also observed a degradation of properties at higher clay loadings. This phenomenon can be due to the phase-separated structures and defects in cross-linked structures. Furthermore, these problems can be caused by the heating phase during the manufacturing process. It is important to mention that in all the references mentioned previously, heating was present during the nanocomposite synthesis procedure.

Another issue that must be addressed is how the natural frequency is affected by the stacking sequence and the boundary conditions. One approach for obtain these relations is the finite element method. Ramtekkar and Desai [31] developed a finite element model based on a six node plane stress mixed element and by applying the Hamilton's energy principle; they were able to obtain the natural frequencies of laminated beams. Their results were in good agreement to data available into the literature. Gubran and Gupta [13] went further, as they demonstrated that natural frequencies are directed affected by the angle ply formation and the stacking sequence. Moreover, the bending-twisting effect is more evident for the angle ply configuration and associated to the Poisson effect and the shear-normal coupling. The largest reduction, $\approx$ 87 %, on the natural frequency is notice when the bending-twisting effect associated to the shear-normal coupling is considered to a 30 degrees angle ply. When the boundary conditions are considered, the natural frequencies present a much more variation.

According to Aydogdu and Timarci [4], when the boundary conditions from simple supported-clamped-simple supported-clamped changed to simple supported-free-simple supported-free a decrease of approximately 400% on frequencies is observed. As mentioned by Lam and Chun [20], when impact loading are considered the target boundary conditions have direct influence on the materials response to low velocity impact tests. Furthermore, Tan et al. [34] verified that clamped laminate plates undergo deflection and stretching during the impact process, while for simply supported conditions stretching does not occur. In other words, when the stress wave produced outward from the impact region reaches the clamped edges, it results in stretching. Another important issue was addressed by Elder et al. [10], whom stated that at low velocity impact the matrix is in general overstressed producing a series of micro-cracking. These local sub-critical cracking does not lead to failure, however it produces a local stress redistribution and energy concentration at the inter-ply regions where the stiffness differences are critical. By assuming these conditions they were able to understand inter-laminar failure into laminated composites under low velocity impact loadings. Likewise, Lin et al. [22] also recognized that for these cases the presence of small amounts of nanoparticles into matrix systems can improve impact properties, as the formation sub-critical cracks mentioned by Elder et al. [10] can be reduced.

The objectives of this paper are twofold. On one hand, low velocity impact tests are conducted to investigate the response of this new polymer-nanoclay-fiber glass nanocomposite. On the other hand, the natural frequencies and damping behavior of this new nanocomposite are examined.

2 Nanocomposites synthesis

The nanocomposite prepared for this investigation is a S2-glass/epoxy-nanoclay. The resin system was chosen owing to its low viscosity and long gel time (60 minutes) at room temperature. The epoxy formulation is based on two parts, part A (*diglycidyl ether of bisphenol A*) and part B - hardener aliphatic amine - (*triethylenetetramine*). The weight mixing ratio suggested by the manufacturer is 100A:20B, and the average viscosity is around 900 cps [8]. The nanoclay particles used in this study are organically modified montmorillonite in a platelet form, while the S-2glass fiber has a plain-weave woven fabric configuration with density of 180 g/m^2 from Texiglass. The S2-glass/epoxy-nanoclay composite is a laminate with 16 layers and 65% fiber volume fraction. This type of laminate configuration is prepared using a vacuum assisted lay-up which leads to an average thickness of 2.4 mm. The amount of nanoclay exfoliated into the epoxy system, in weight, is 1%, 2%, 5% and 10%, respectively. The nanoclay properties listed in Table 1 are from Subramaniyan et al. [32]. Moreover, a set of S2-glass/epoxy laminated composite without nanoclay is prepared to serve as comparative basis. For each group at least five specimens is prepared and tested.

Table 1: Nanoclay properties from reference [32]

Mean dry particle size [μm]	**Average platelet thickness [nm]**	**Mineral Purity [% min]**	**Moisture [%max]**	**Specific density [g/cm^3]**
8-10	49	98	3	1.71

The nanocomposite synthesis involves two different steps, i.e. the nanoclay exfoliation procedure and the lamination practice. As stated by Yasmin et al. [36], the exfoliation process can be done by direct mixing, sonication mixing, shear mixing or a combination of sonication and shear mixing. Additionally, they affirm that shear mixing is more appropriate to the exfoliation of expanded graphite, while direct mixing is more suitable for ceramic nanoparticles. In the present study, the nanoclay exfoliation process is performed by stepwise direct mixing, in other words, the nanoclay particles are mixed to acetone and later on the solution, acetone/nanoclay, is blended into the hardener. As the hardener has a much lower viscosity, the homogenization procedure is easier. Moreover, there is no need for a stirring process as in Yasmin et al [35, 36] Subramaniyan et al [32], and Liu et al [22], for instance. However, as the blended process generates a foaming solution the degassing step is required. As observed by Avila et al. [3], the presence of acetone leads to a much slower cure and in some cases, the cure process is partially inhibited. Therefore, the degassing process is used not only to eliminate the bubbles but also to allow the acetone evaporate.

After degassing for an hour, the solution (hardener+acetone+nanoclay) becomes clear of

any particle agglomeration and bubbles. However, the addition of nanoclays turns a usually translucent resin into an opaque one. The solution is then mixed to the resin. The next step is a conventional stacking sequence and vacuum assisted wet lay-up lamination. After twenty-four hours of cure under vacuum at room temperature, a co-cure procedure is applied. According to Kim and Daniel [19], residual strains and stresses can be induced by the cure/co-cure procedures. Likewise, for the present case, the cure kinetic is highly dependent on peak temperature, increase/decrease rates, and the components mixed, i.e. resin, hardener, nanoclay and acetone. Based into these data, and the previous results reported by Avila et al. [3], the co-cure method at low temperature was selected.

3 Testing procedures: low velocity impact and vibration

Once the S2-glass/epoxy-nanoclay is prepared, the impact resistance test by falling dart can be performed. Following the ASTM D 5628-01 [1], the dart has a hemispherical nose with a radius of 10.0±0.1 mm. The testing device is described by the schematic diagram represented in Figure 1, while the specimen clamp is a two-piece rectangular specimen with a central circular cutout of 100.0±0.1 mm. The dart has a weight of 246 grams and six additional steel circular plates with a diameter of 75.0±0.1 mm and a thickness of 15.0±0.1 mm. They can be placed into the rod linked to the dart. The average weight of each circular plate is 528 grams. As stated by Belingardi and Vadori [5], the velocity in a low velocity impact test, such as the one described in ASTM D 5628-01 [1] standard, can be calculated by the expression:

$$v = \sqrt{2g\Delta h} \tag{1}$$

where v is the velocity, g is the gravity acceleration and Δh is the difference in height.

As the drop weight tower has a maximum height of 3.0 meters, the limiting velocity for the device is 7.67 m/s. The dart is made of AISI 4330 steel. Moreover, the six steel disks can be assembled individually into the dart leading to a mass variation from 246 to 3414 grams. As recognized by Lam and Chun [20], material response is also affected by the target boundary conditions. Therefore, this investigation considers not only the clamped condition, but also the simply supported one. The clamped condition is guaranteed by the usage of four bolts as shown in Figure 1. Furthermore, an additional investigation on how the amount of nanoclay exfoliated affects the natural frequency and the damping coefficient is also carried out, as those parameters have influence on perforation behavior as stated by Cantwell et al. [6].

The vibration analysis is performed using a Hewlett Packard 35670A vibration analyzer associated to a power amplifier type 2170 from Bruel & Kjaer. The mini shaker type 4810 is also from Bruel & Kjaer, while the vibration transducers are from Piezoeletronics Incorporated. The plates have the same dimensions as those used into impact tests. To be able to investigate the nanoparticles influence into vibration analysis, samples with 0%, 1%, 2%, 5% and 10% of nanoclay with respect to the matrix weight is employed. The fiber volume fraction is kept

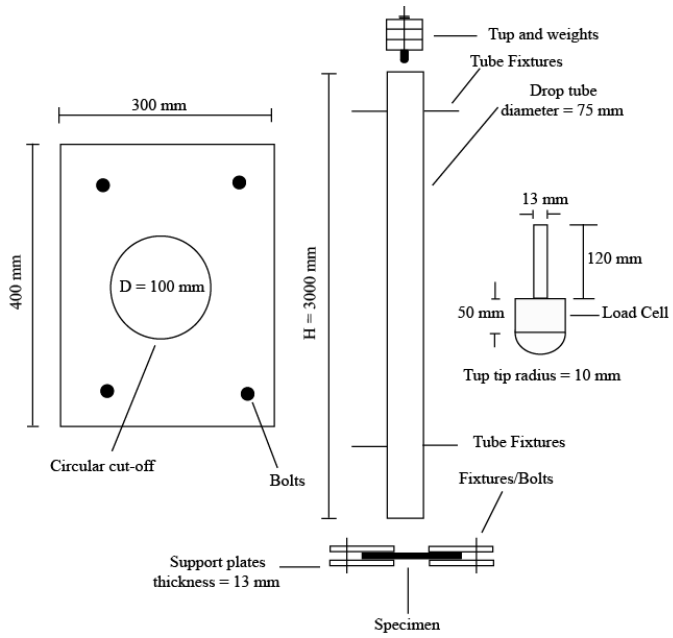

Figure 1: Falling mass impact tester – schematic diagram

constant and around 65%.

4 Data analysis and considerations

In this study two boundary conditions are considered, i.e. clamped and simply supported, two different heights and weights. These conditions lead to six levels of impact energy and a total of twelve distinct conditions. They are combined in Table 2.

Table 2: Impact experiment conditions

Energy Level ID	**#1**	**#2**	**#3**	**#4**	**#5**	**#6**
Boundary Conditions	Clamped and SS*			Clamped and SS*		
Height [m]	2.0	2.0	2.0	3.0	3.0	3.0
Velocity [m/s]	6.26	6.26	6.26	7.67	7.67	7.67
Mass [g]	780.0	1308.0	1840.0	780.0	1308.0	1840.0
Energy[J]	15.30	25.67	36.10	22.96	38.49	54.15

* Simple Supported

The nanocomposite performance is evaluated by three parameters, i.e. the front face de-

laminated area, the back face failure area and deflection. The front face delaminated area is calculated by assuming the front mark as an elliptical shape. For practical purposes, the Hart-Smith [15] optimal octagonal shape approximation, case 2 of Figure 2, is employed, while the back face failure area is computed either by a rectangular or circular shape area. Notice that according to Sutherland and Soares [33], instead of using a C-Scan as these specimens are translucent, it is possible to view the damage simply by back-lighting the plates. This gives the approximate damage area, and also a qualitative description of the damage.

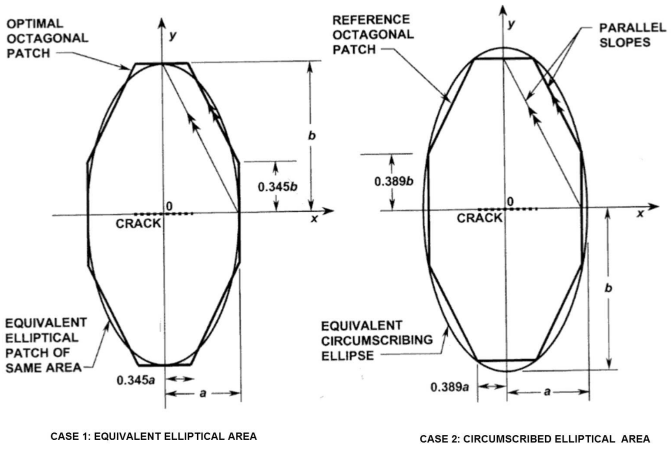

Figure 2: Optimal octagonal shape employed. Modified from reference 33

Figures 3A-3C show the three parameters studied as a function of the impact energy. As expected the front face delaminated areas are higher for the clamped condition than the ones from the simply supported. For the same impact energy, the front face delaminated area is reduced by approximately 22% with the addition of 1 %wt of nanoclay to the epoxy system for both cases, i.e. clamped and simply supported conditions. However, the front face failure area increases when the dart rebound phenomenon is noticed. A possible reason for these rebounds can be associated to the matrix brittle/ductile transition behavior. Nanoclays are associated with the molecular links creating a matrix less brittle than the original one, which can lead to a rebound without a critical failure. Figures 4A-4B show the rebound marks for two levels of impact energy, 15.30 and 25.67 J, respectively. In some cases the rebound is observed during the impact but the marks are too close to be perceived as shown in Figure 4C.The back face failure area and back face deflection are much smaller in nanocomposites. For low impact energy levels, i.e. 15-22 J, the area reduction is around 10 % while the back face deflection is reduced by approximately 45%. In middle range impact energy, i.e. 25-36J, the back face failure area is decreased by 21%, while its deflection is reduced by 20%. Finally, in high range impact energy level, i.e. 38-54 J, a small decrease $\approx$ 10% is observed into front face delaminated area, while the back face failure area experiments an increase for clamped conditions. The back face deflection, however, indicates an increase in its values for clamped conditions. This can be evidence of load

concentration.

Notice that back side marks bear resemblance to those presented by Lemanski et al. [21]. However, the cross shape mark is more pronounced within those nanocomposites. As it can be observed in Figures 4A-4B, the primary impact causes a larger damage which includes a rear face deflection, while the secondary impact (rebound) cause no back faces deflection. By applying the dimensionless analysis proposed by Nurick et al. [29] for blast loadings, it is possible to conclude that for secondary impact the back face dimensionless deflection approaches zero, which can be evidence that most of the energy is absorbed during the primary impact. To be able to understand the energy absorption mechanism the damping coefficient for each group of plates has to be investigated.

To know how the nanomodified epoxy matrix affects the overall nanocomposite behavior, a set of impact test is performed. In this phase of research, the amount of exfoliated nanoclay is 0%, 1%, 2%, 5% and 10% wt, respectively. A set of at least three of impact plates were prepared for simply supported and clamped conditions, while the energy employed is approximately 40 J. As it can be observed in Figures 5A-5C as the amount of exfoliated nanoclay is increased the damping is also improved. Furthermore, when the rate of rebound force reduction is analyzed, it is possible to conclude that it is directly proportional to the amount of exfoliated nanoclay, as it can be observed in Figure 5C. However, it seems that the optimum amount of exfoliated nanoclay is 5%. Higher nanoclay concentrations can lead to excessive stiffness which leads to more rebounds, but a wave propagation investigation is also required.

The next step is the vibration analysis. According to Gibson [11], a typical frequency/response function for impulse test allows the definition of the natural frequencies. Additionally, the peaks in the frequency/response spectrum are the location of natural frequencies of the specimens. Figure 6 shows these frequencies response for the specimens tested, while in Figure 7 the coherence plot is represented. Meanwhile, Table 3 summaries not only the natural frequencies but also the damping coefficients associated.

Table 3: Vibration parameters

Nano %									
0		**1**		**2**		**5**		**10**	
f **[Hz]**	C $\mathbf{10^{-3}}$	f **[Hz]**	C $\mathbf{10^{-3}}$	f **[Hz]**	C $\mathbf{10^{-3}}$	f **[Hz]**	C $\mathbf{10^{-3}}$	f **[Hz]**	C $\mathbf{10^{-3}}$
181.50	38.72	180.50	36.41	181.00	35.10	192.00	33.30	177.50	36.84
386.00	14.86	375.50	17.91	389.50	14.44	399.00	15.18	395.00	16.51
528.50	13.70	508.00	24.12	526.00	15.39	547.50	13.27	533.50	27.40
619.50	15.40	607.50	12.65	622.00	14.27	643.50	12.46	620.50	14.19
759.50	13.68	745.50	14.41	768.50	15.84	781.00	16.78	771.00	18.17

As it can observed in Table 3, there is no significant changes on natural frequencies (f) with the addition nanoparticles up to 2%. The same behavior can be observed with respect to the

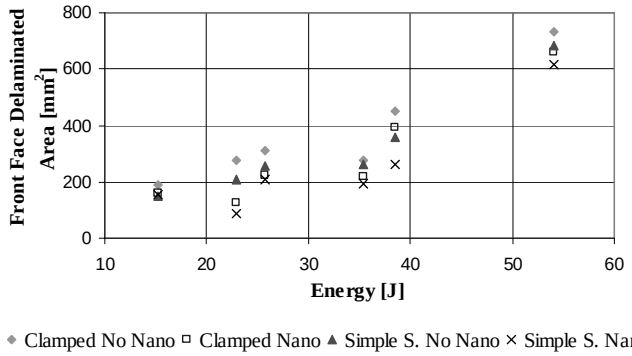

(a) Front face delaminated area

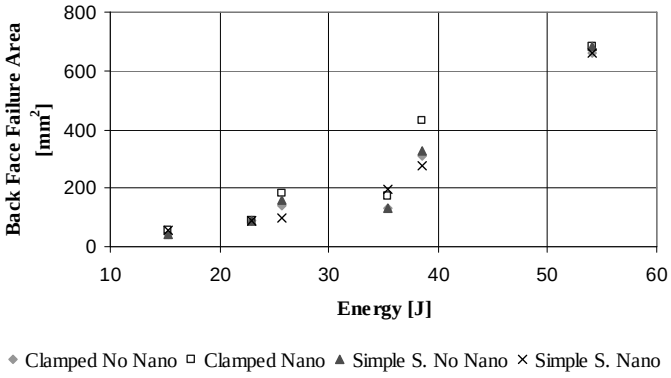

(b) Back face delaminated area

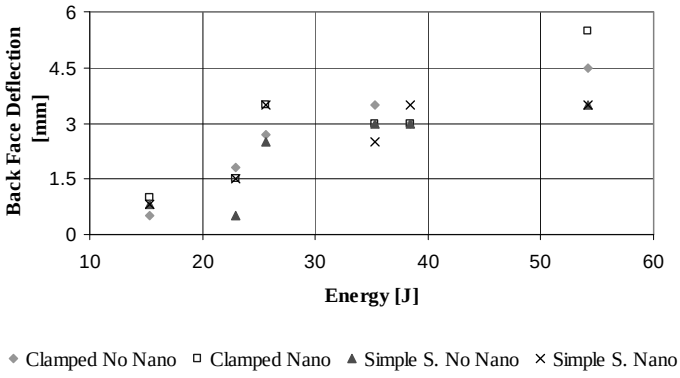

(c) Back face failure deflection

Figure 3: Comparative study - Conventional versus Nanocomposites

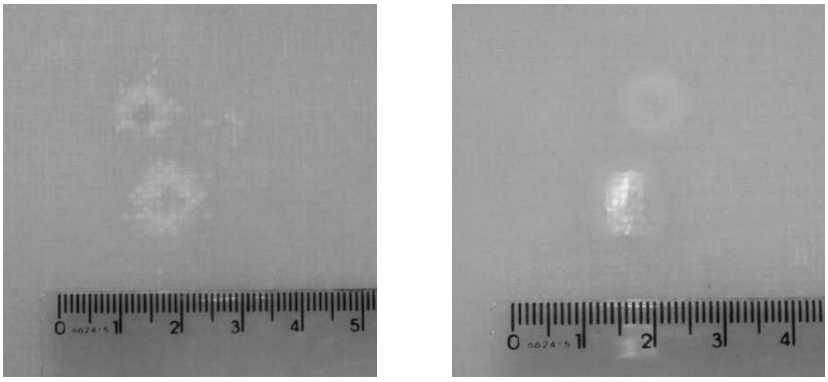

(a) Front and back faces, damage marks - Energy level #1

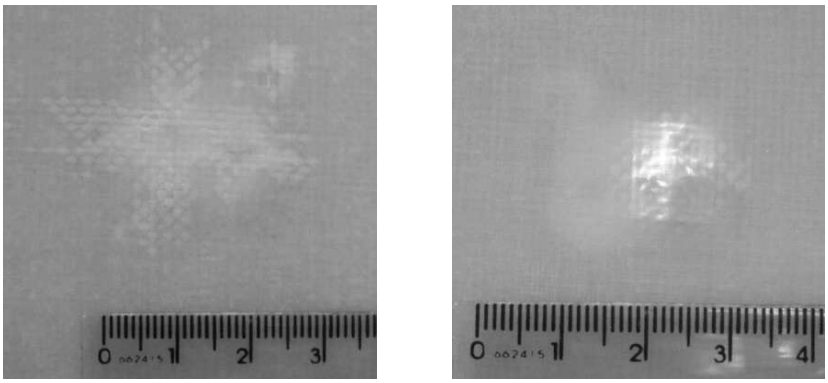

(b) Front and back faces, damage marks - Energy level #2

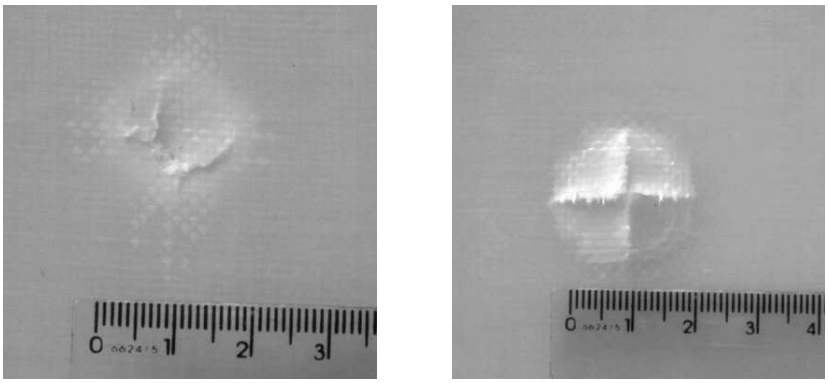

(c) Front and back faces, damage marks - Energy level #5

Figure 4: Impact marks at front and back sides of nanocomposites

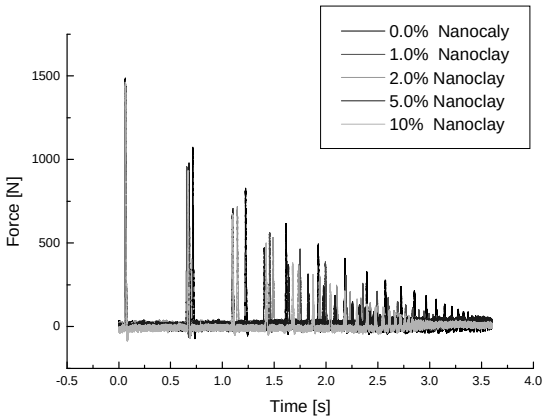

(a) Load-time history

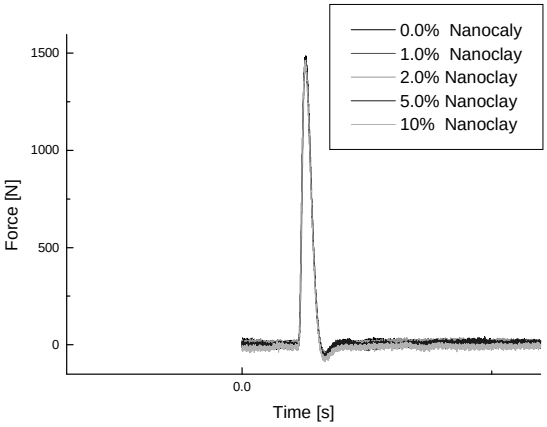

(b) Zoom showing the 1^{st} impact peak at load-time history chart

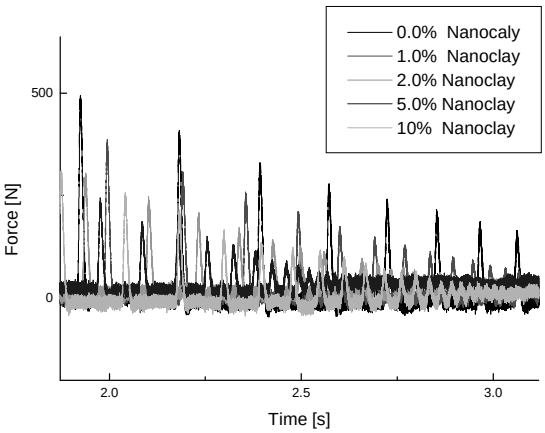

(c) Zoom showing the damping enhancement

Figure 5: Load-time history charts

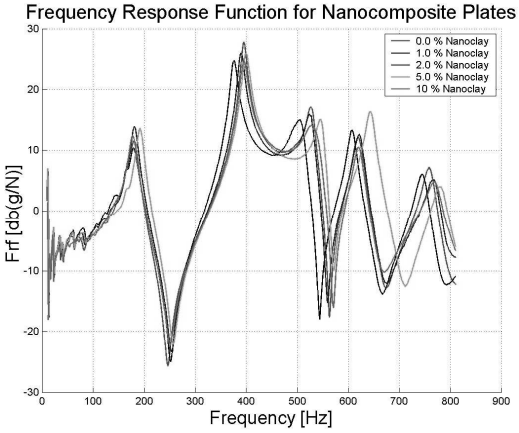

Figure 6: Frequency/response function for impulse

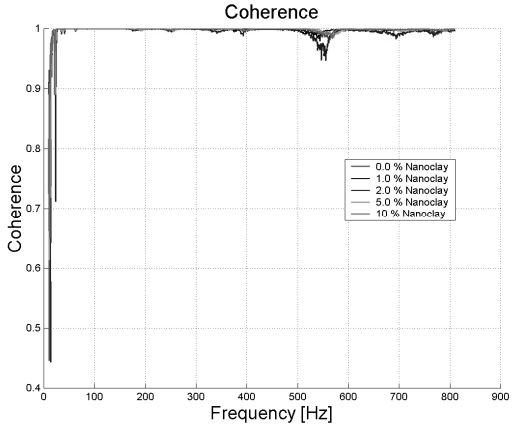

Figure 7: Coherence plots

damping coefficient. No significant variations on natural frequencies, difference around 1.5%, are observed when the nanoparticles content reaches 10%, as it can be seen in Table 3. This can be due to the fiber plain weave configuration, which leads to a "preferential path" for the waive propagation. However, for the 5^{th} vibration mode the damping coefficient (C) experiences an increase close to 32%. Considering that the stacking sequence is the same the only reason for this increase is the nanoparticle presence. This better performance can be partially explained by the increase on stiffness reported by many authors, e.g. Avila et al. [3], Yasmin et al. [35,36] and Subramaniyan et al. [32].

Assuming that there is no significant variation on wave propagation velocity with the amount of nanoclays exfoliated into the nanocomposite, the failure mechanism during the impact tests must be associated not only to the damping coefficient but also stiffness and toughness variations. As this research deals with two different levels of reinforcement, one at nanoscale, nanoparticles inside the matrix/resin, and another at microscale, fiber reinforcement with plain weave configuration, it is possible to conclude that coupling between nano and micro effects can be a key issue in this problem. The fibers can be assumed as a primary "road map" for weave propagation while leads to a near constant natural frequency and damping coefficient. At same time, the nanoclay presence increases the matrix toughness and stiffness. However, the increase on stiffness does not affect the wave propagation as the primary wave path is still the same.

Nevertheless, when the four edges clamped condition is imposed the wave propagation and modes superposition lead to an increase on damping parameters, as Figures 5A-5C demonstrate. The coupling between different vibration modes in a confined space could be the reason for this better performance. When the impact energy is reduced, $\approx$ 20J, and the impact areas are studied a set of conclusions can be drawn. It seems that nanomodified epoxy is more efficient that conventional one. By analyzing Figures 8A-8C, a clear pattern is observed, i.e. the impact strength increases with the nanoclay presence. However, the impact strength seems to increase gradually with the nanoclay content. When the nanoclay content reaches 10% the delaminated area drops drastically. Moreover, not only the back delaminated area decreases but also the back face deflection. In fact, for the 10% nanoclay content although delamination phenomenon is present, no back face deflection is observed. When a comparison is done considering the composite's front delaminated area with net resin and 10 % nanoclay content the conclusion is that a decrease of 50% can be observed. The presence of nanoclays could lead to an increase on matrix toughness due to stronger molecular crosslink. However, other mechanisms, e.g. changing into damping coefficient and natural frequencies, can be present and associated to the enhancement of impact resistance properties

5 Closing comments

The exfoliation of nano-sized clays increases the composite impact strength, as the damaged area is decreased by approximately 20% for small amounts of nanoclay contents. However, when the

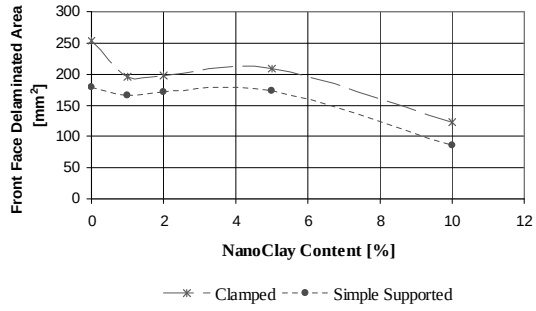

(a) Front face delaminated area

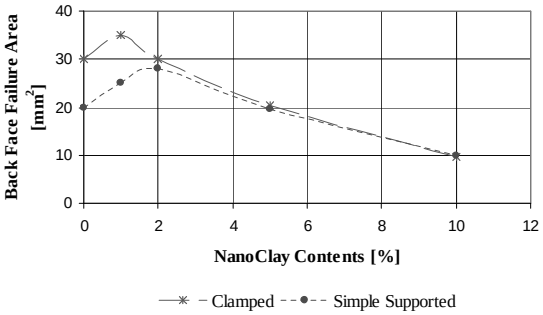

(b) Back face delaminated area

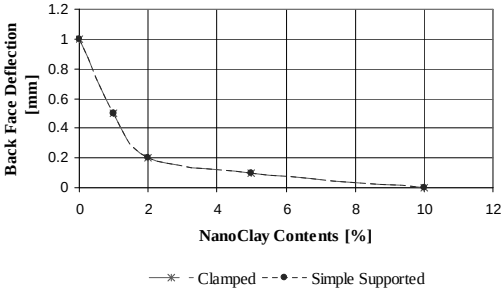

(c) Back face deflection

Figure 8: Nanoclay contents versus damaged area.

concentration reaches around 10% the increase on impact strength is close to 50%. Moreover, the rebound/spring effect is also noticed in all cases where the nano-sized clay is applied with superior performance when compared against conventional composites.

The natural frequencies and the damping coefficient were experimentally determined for the new laminated nanocomposite. A small variation on natural frequencies was observed when the amount of nanoparticles is exfoliated into the matrix. The damping coefficient is practically constant, the only variation observed was for the 781 Hz frequency (5^{th} vibration mode for nanocomposite with 10% nanoparticle content) shows and increases around 30% with respect to the nanocomposite without nanoparticles. As the impact toughness is increased by the exfoliated nanoparticles. Therefore, it is reasonably to suppose that a more complex phenomenon is present.

When the four edges clamped condition is imposed the overall composite damping is increased with the nanoclay concentration. This can be due to the vibration mode superposition associated to a stiffness enhancement. However, the optimal nanoclay concentration seems to be 5%. A possible explanation for this phenomenon is the excessive increase on stiffness for the 10% nanoclay concentration, which leads to a decrease on damping. A more comprehensive investigation is under development to understand the mechanisms among the different scales os analysis, i.e. nano-, micro- and macro-mechanics.

Acknowledgements: The authors would like to acknowledge the financial support provided by the Brazilian Research Council (CNPq).

References

[1] ASTM D 5628-01. Standard test method for impact resistance of flat, rigid plastic specimens by means of a falling dart (tup or falling mass), Annual Book of ASTM Standards, New York (NY, USA). *ASTM Press*, 8(2):628–637, 2001.

[2] S. Abrate. *Impact on Composite Structures*. Cambridge UP, Cambridge, 1998.

[3] A.F. Avila, M.I. Soares, and A. Silva Neto. An experimental investigation on nanocomposites under impact loading. In M. Alves and N. Jones, editors, *Impact Loading of Lightweight Structures*, pages 89–102, Florianopolis (Santa Catarina, Brazil), 2005. WIT Press.

[4] M. Aydogdu and T. Timarci. Vibration analysis of cross-ply laminated square plates with general boundary conditions. *Composites Science and Technology*, 63(5):1061–1070, 2003.

[5] G. Belingardi and R. Vadori. Low velocity impact tests of laminate glass-fiber-epoxy matrix composite material plates. *Int J Impact Engng*, 27(2):213–229, 2002.

[6] W.J. Cantwell, H. Kiratisaevee, and Md.A. Hazizan. The low velocity impact response of high-performance sandwich structures. In M. Alves and N. Jones, editors, *Impact Loading of Lightweight Structures*, pages 135–146, Florianopolis (Santa Catarina, Brazil), 2005. WIT Press.

[7] W.L. Cheng, S. Langlie, and S. Itoh. High velocity impact of thick composites. *Int J Impact Engng*, 29(2):167–184, 2003.

[8] Huntsman Chemical Company. Huntsman chemical co. araldite data sheet. pages 1–16, 2004.

[9] G.A.O. Davies and X. Zhang. Impact damage prediction in carbon composite structures. *Int J Impact Engng*, 16(1):149–170, 1995.

[10] D.J. Elder, R.S. Thomson, M.Q. Nguyen, and M.L. Scott. Review of delamination predictive methods for low speed impact of composite laminates. *Composite Structures*, 66(7):677–683, 2004.

[11] R.F. Gibson. Modal vibration response measurements for characterization of composite materials and structures. *Composites Science and Technology*, 60(10):2769–2780, 2000.

[12] B. Gu. Analytical modeling for ballistic perforation of planar plain-woven fabric target by projectile. *Composites Part B*, 34(3):361–371, 2003.

[13] H.B.H. Gubran and K. Gupta. The effect of stacking sequence and coupling mechanisms on natural frequencies of composite shafts. *Journal of Sound and Vibrations*, 282(2):231–248, 2005.

[14] A. Haque and M. Shamsuzzoha. S2-glass/epoxy polymer nanocomposites: manufacturing, structures, thermal and mechanical properties. *Journal of Composite Materials*, 37(20):1821–1837, 2003.

[15] L.J. Hart-Smith. A demonstration of the versatility of rose's closed-form analysis for bonded crack-patching. In L. Repecka and F.F. Sameri, editors, *Proceedings of the 46th International SAMPE Symposium*, pages 1118–1134, Long Beach (California, USA), 2001. SAMPE Press.

[16] N. Hu, H. Sekine, H. Fukunaga, and Z.H. Yao. Impact analysis of composite laminates with multiple delaminations. *Int J Impact Engng*, 22(7):633–648, 1999.

[17] I. Isik, U. Yilmazer, and G. Bayram. Impact modified epoxy/montmorillonite nanocomposites: synthesis and characterization. *Polymer*, 44(25):6371–6377, 2003.

[18] J.E.L. da Silva Junior, S. Paciornik, and J.R.M. d'Almeida. Evaluation of effect of ballistic damaged area on the residual impact strength and tensile stiffness of glass-fabric composite materials. *Composite Structures*, 64(1):123–127, 2004.

[19] Y.K. Kim and I.M. Daniel. Cure cycle effect on composite structures manufactured by resin transfer molding. *Journal of Composite Materials*, 36(14):725–1743, 2002.

[20] K.Y. Lam and L. Chun. Analysis of clamped laminated plates subjected to conventional blast. *Composite Structures*, 29(2):311–321, 1994.

[21] S.L. Lemanski, G.N. Nurick, M.C. Simmons, G.S. Langdon, W.J. Cantwell, and G.K. Schleyer. Quantifying the behavior of fiber metal laminates subject to localized blast loading. In M. Alves and N. Jones, editors, *Impact Loading of Lightweight Structures*, pages 321–334, Florianopolis (Santa Catarina, Brazil), 2005. WIT Press.

[22] J-C. Lin, L.C. Chang, M.H. Nien, and H.L. Ho. Mechanical behavior of various nanoparticle filled composites at low-velocity impact. *Composite Structures*, 2005 to appear.

[23] D. Liu, B.B. Raju, and X. Dang. Impact perforation resistance of laminated and assembled composite plates. *Int J Impact Engng*, 24(8):733–748, 2000.

[24] T. Liu, K.P. Lim, W.C. Tjiu, K.P. Pramoda, and Z-K. Chen. Preparation and characterization of nylon 11/organoclay nanocomposites. *Polymer*, 44(27):3529–3535, 2003.

[25] R.K. Luo, E.R. Green, and C.J. Morrison. Impact damage analysis of composite plates. *Int J Impact Engng*, 22(5):435–447, 1999.

[26] R.A.W. Mines, A.M. Roach, and N. Jones. High velocity perforation behavior of polymer composite laminates. *Int J Impact Engng*, 22(6):561–588, 1999.

[27] M.F.S.F. Moura and J.P.M. Gonçalves. Modeling the interaction between matrix cracking and delamination in carbon-epoxy laminates under low velocity impact. *Composites Science and Technology*, 64(9):1021–1027, 2004.

[28] N.K. Naik and P. Shrirao. Composite structures under ballistic impact. *Composite Structures*, 66(8):578–590, 2004.

[29] G.N. Nurick, M.E. Gelman, and N.S. Marshall. Tearing of blast loaded plates with clamped boundary conditions. *Int J Impact Engng*, 18(6):802–827, 1996.

[30] S.V. Potti and C.T. Sun. Prediction of impact induced penetration and delamination in thick composite laminates. *Int J Impact Engng*, 19(1):31–48, 1997.

[31] G.S. Ramtekkar and Y.M. Desai. Natural vibrations of laminated composite beams by using mixed finite element method. *Journal of Sound and Vibration*, 257(4):635–651, 2002.

[32] A.K. Subramaniyan, Q. Bing, D. Nakaima, and C.T. Sun. Effect of nanoclay on compressive strength of glass fiber composites. In B.V. Sankar, editor, *Proceedings of the 18th ASC/ASTM Joint Technical Conference*, Gainesville (Florida, USA), 2003. Florida UP. CDROM.

[33] L.S. Sutherland and C.G. Soares. Impact test on woven-fabric e-glass/polyester laminates. *Composites Science and Technology*, 59(9):1553–1567, 1999.

[34] V.B.C. Tan, V.P.W. Shim, and T.E. Tay. Experimental and numerical study on response of flexible laminates to impact loadings. *International Journal of Solids and Structures*, 40(22):6245–6266, 2003.

[35] A. Yasmin, J.L. Abot, and I.M. Daniel. Processing of clay-epoxy nanocomposites by shear mixing. *Scripta Materialia*, 49(1):81–86, 2003.

[36] A. Yasmin, J-J. Luo, and I.M. Daniel. Processing of graphite nanosheet reinforced polymer nanocomposites. In E. Armeiros, editor, *Proceedings of the 19th ASC/ASTM Joint Technical Conference*, Atlanta (Georgia, USA), 2004. Georgia Institute of Technology UP. CDROM.

[37] D-R. Yei, S-W. Kuo, Y-C. Su, and F-C. Chang. Enhanced thermal properties of ps nanocomposites formed from inorganic poss-treated montmorillonite. *Polymer*, 45(22):2633–2640, 2004.